JOINT EUROPEAN TORUS

JET–P(91)37

M. Bures, J. Jacquinot, M. Stamp, D. Summers, D.F.H Start, T. Wade,
D .D'Ippolito, J. Myra and JET Team

Assessment of Beryllium Faraday Screens of the JET ICRF Antennas

Assessment of Beryllium Faraday Screens of the JET ICRF Antennas

M. Bures, J. Jacquinot, M. Stamp, D. Summers, D.F.H Start, T. Wade,
D .D'Ippolito[1], J. Myra[1] and JET Team*

JET-Joint Undertaking, Culham Science Centre, OX14 3DB, Abingdon, UK

[1]Lodestar Research Corporation, Boulder, Colorado, USA
** See Appendix 1*

Preprint of Paper to be submitted for publication in
Nuclear Fusion

Assessment of Beryllium Faraday Screens of the JET ICRF Antennas.

M.Bureš, J.Jacquinot, M.Stamp, D.Summers, D.F.H.Start, T.Wade.
JET Joint Undertaking, Abingdon, Oxon, OX14 3EA, UK.

D.D'Ippolito, J.Myra
Lodestar Res. Corp., Boulder, Colorado, USA.

Abstract.

The installation of beryllium(Be) Faraday screens(FS) at the ICRF antennas in JET resulted in elimination of the RF specific effects on the plasma boundary by the impurity influx originating at the screens. In dipole phasing, k_{II}=7 m^{-1}, the influx is for all purposes negligible. In monopole(k_{II}= 0 m^{-1}) the beryllium influx does not exceed ϕ_{Be}^{FS}= 1 x 10^{19} atoms $MW^{-1}s^{-1}$ and corresponding $\delta Z_{eff}/P_{RF}$< 0.005 MW^{-1}. The observed dependences of the ϕ_{Be}^{FS}(in monopole phasing) on plasma density, antenna voltage, antenna phasing and the angle between FS elements and the magnetic field in the boundary $\vec{B}(a)=\vec{B}_{\theta}(a)+\vec{B}_{T}(a)$ confirm that the release mechanism is the sputtering by the ions accelerated in the RF–enhanced Bohm–Debye sheaths forming at the front face of the FS. When the angle between FS and the $\vec{B}(a)$ is ≈ 22 degrees the fraction of the RF power radiated by the antenna, dissipated at the screen, can reach 40%. At high antenna voltage the arcing across the FS can occur. With dipole phasing the heating efficiency is not degraded even with the large angle and all the power coupled by the antenna is absorbed at the resonance position near the plasma centre. The open screen design did not introduce any disadvantages. The experience from the JET operation at powers up to 22 MW shows that, if the necessary conditions are met, i.e., RF rectification is minimised and material with the low sputtering coefficients at energies 0.5–1keV is used, then the influx from the FS is eliminated.

1.0 Introduction.

At the start of the 1990 experimental campaign on JET, the ICRF antennas of the RF heating system were equiped[1,2] with all–beryllium Faraday screens(FS). The reasons for replacing old nickel screens were the following: 1)to eliminate the nickel influx from the FS observed[3,4] when the antenna is active, 2)to simplify the design and to avoid the requirement for active cooling of the FS during long heating pulse operation and 3)to test the open FS design. Previously, a good performance has been achieved with the old nickel FS by the beryllium gettering of the FS front–face. The detailed study of the beryllium influx from the FS led to understanding of the physical processes responsible for the influx release[5,6]. It was found that the RF field rectification at the Bohm–Debye sheaths, originally suggested by Perkins[7], can produce quasi–dc potentials of ≈ 0.5 keV and sometimes higher. The ions, accelerated by such potentials, will impinge on the surface of the FS at an energy close to the maximum of the sputtering yield. In some cases(Ni, Cr, Mo for example) the yield will exceed unity. Such condition will lead to an important impurity release and a subsequent pollution of the other internal surfaces of the tokamak. To eliminate the FS influxes number of conditions have to be met[5,6]. **First**, the RF rectification process should be minimised by

1)aligning the FS elements with the magnetic field at the plasma boundary

2)lowering the plasma density at the FS surface by using the side protection tiles

3)dipole(current straps out of phase) antenna phasing (k_{II}= $7m^{-1}$ on JET)

4)low antenna power density(low voltage per screen element).

Second, the effects of the RF rectification and subsequent ion acceleration and ion sputtering should be minimised by using low Z material with the low deuterium sputtering and selfsputtering yields.

During the tests of the new beryllium screens the previously observed dependences(listed above) on antenna voltage, edge density, antenna phasing and the FS/$\vec{B}$(a) angle were studied.

2.0 Experimental arrangements.

The JET device is a low aspect ratio tokamak with major radius R=3m and minor radius a=1.2 m. In the series of experiments reported in this paper, the plasma was operated in a beryllium limiter configuration with a toroidal field on axis B_0 =2.9 and 2.2 T respectively and plasma current I_p= 3 MA. The data refer to two cases of the direction of the toroidal field. The basic scans with the RF power and plasma density were done with the normal direction of the toroidal field and the value of toroidal field on axis B_0=2.9 T. In that case the angle between the FS elements and the magnetic field in the plasma boundary was small, typically less than 5 degrees. With the toroidal field reversed, the angle was ≈22 degrees. Heating scenario was the D(H) minority heating with the minority species indicated in the bracket. The frequency was chosen such that the wave was damped at the minority cyclotron resonance on axis. The antennas were phased either as monopoles or dipoles. The angle of the FS elements, at which they are installed, is θ_0 ≈15 degrees with respect to the toroidal field. The details of the design features of the new beryllium screens are described in a publication by Walker et al.[8] and the photograph of the antenna equipped by the beryllium screens is shown in ref.[2].

The beryllium influxes from the FS were measured by monitoring intensity of visible lines BeI and BeII. It was shown earlier[6] that BeI, even as a raw signal, represents the neutral influx with an acceptable accuracy. The BeII is more sensitive than BeI but the signal may include a contribution which is not related to the influx from the screen. The data collected with the normal direction of the toroidal field were taken at the beginning of the experimental campaign. The data with the toroidal field reversed were obtained much later. This is an important aspect because the state of the FS surface relates to the amount of the deposited carbon. The inspection of the screens, after the end of the experimental campaign, has shown that a deposition of carbon takes place. Carbon originates at the upper x–point target tiles which are eroded by large power fluxes during the plasma discharges with the x–point inside the vessel.

3.0 Experimental results.

3.1 Normal direction of toroidal field.

The **RF specific** influxes from the FS, ϕ^{FS}, take place on a fast(τ<10 ms) time scale[5]. A convenient way to identify the influx is to modulate the RF power by square wave and to measure the corresponding fast response. In Fig.1 the intensity of BeII is plotted as a function of time for two different shots with modulated RF power. The power evolution was similar in both shots, modulated at 2 Hz with maximum power increasing in 4 steps. The two discharges were run at different plasma density. It can be concluded that, as expected, the beryllium influx increases with RF power(or antenna voltage), its response is fast and it scales with plasma density. The dependence of FS influxes on the plasma density implies that the FS edge density is proportional to the plasma density. The $n_e^{EDGE} \propto <n_e>^{\beta}$ dependence is generaly observed[9] and at high densities β >1. It is interesting to note that the level of the background signal(measured before the application of RF power) is rather high. It can be attributed to the background Bremstrahlung and the beryllium ions not originating at the FS. Summary of the BeII data is shown in Fig.2. The influx is shown to scale with the RF voltage of the powered antenna and the plasma density. To infer the precise scaling is not possible because the voltage and the density range are rather restricted. To test the dependence of the ϕ_{Be}^{FS} on the angle α, defined as:

$$\alpha = |\theta_o - \theta| = |\theta_o \pm a/Rq|; \quad -B_T \text{ normal}, \; +B_T \text{ reversed}$$

where q is the safety factor at the plasma boundary, the plasma current was ramped from 3 to 5 MA and back to 3 MA as shown in Fig.3. Such a ramp iplies a variation of the angle α in the range $\approx$ 0–4 degrees. It proved to be difficult to keep the other plasma parameters constant during the curent ramp and in particular the elongation. As a consequence the antenna–plasma distance increases with plasma current (see also the corresponding change of the coupling resistance R_c) and the resulting BeII behaviour is dominated by the density changes at the screen. In particular a very steep

increase in the BeII signal, correlated to the R_c(and therefore n_{edge}), is observed during the time interval 14–16s.

A quantitative estimate of the ϕ_{Be}^{FS} was derived by comparing the BeI signal with the previously calibrated[6] BeI data. The circles plotted in Fig.4 represent the measurements on the Be screen. The restriction on the voltage was imposed by the surface contamination of the insulator of the antenna electrical feed–through. It can be seen that the level of influx is in the same range as that observed from the beryllium gettered nickel screens[6], i.e., $\phi_{Be}^{FS} < 1 \times 10^{19}$ atoms $MW^{-1}s^{-1}$ implying $\delta Z_{eff}/P_{RF} < 0.005\ MW^{-1}$. These results were anticipated because the geometry of the screen did not change. During the progress of the experimental campaign an increasingly larger fraction of the JET discharges was run in the x–point configuration. Erosion of the x–point target plates, due to the high power input by the NBI and RF systems, implies large carbon fluxes which are subsequently deposited on the internal surfaces of the vessel. Deposition on the FS was also observed. This explains the low BeI signal level(Fig.4) during the latter part of the experimental campaign. It is possible that, at that stage, a fraction of ϕ^{FS} constituted an influx of carbon. The nickel influx was, of course, entirely eliminated and high quality H–modes with RF heating alone were obtained. It was concluded [10] that the impurity influxes across the plasma boundary play a key role in the quality of the H–modes in terms of both energy and particle confinement.

3.2 Reversed direction of toroidal field.

The efficiency of ICRF heating is substantially reduced when the direction of the toroidal field is reversed while the RF antennae are phased as monopoles. In Fig.5 the plasma stored energy is plotted as a function of input power. Results with the dipole configuration are compared to the degraded performance with monopoles. It was previously shown[11] that, with normal field direction, the heating efficiency is approximately independent of antenna phasing. Also, there is no reason to assume that the plasma confinement properties vary with antenna phasing. Rather the lower

heating efficiency can be explained by the dissipation of a large fraction of the antenna power in the RF–enhanced sheaths at the FS. To estimate the fraction of this power P_{FS} is straight forward;

$$P_{FS} = \frac{P_{RF}(\tau_{INC}^{Dip} - \tau_{INC}^{Mon})}{\tau_{INC}^{Dip}}$$

Here τ_{INC} is defined as the slope $\delta W/\delta P$ and P_{RF} is the net RF power radiated across the surface of the FS. It is derived from the generator output power P_{GEN} and corrected for the ohmic losses of the transmission line–antenna system. Thus

$$P_{RF} = \eta P_{GEN}$$

$$\eta = (R_c - R_v)/R_c$$

where R_c is the antenna coupling resistance measured in the presence of the plasma while R_v is measured in the vacuum. The incremental confinement time, measured with dipoles, has a value $\tau_{INC}^{Dip} \approx 0.35$s which is an average value typically observed. The incremental confinement with monopole phasing, $\tau_{INC}^{Mon} \approx 0.2$s implies that the fraction of the power dissipated at the screen can be as high as ≈40%. An order of magnitude estimate of the power dissipated per FS element published earlier[12] for the case of sputtering in the gaps between the FS elements as proposed in references[7, 12, 13, 14].

In the present case the contribution to the screen sputtering and the corresponding power dissipation come predominantly from the front face of the screen[5, 6]. Then the modified expression for the power dissipated in the sheaths on the FS surface is

$$P_{FS} = 1.5 \times 10^{-15} \Sigma\, A \sin\gamma\, n_{io}\, Z\phi_o\, (ZT_e/\mu)^{1/2} \qquad (1)$$

where the units of power are P_{FS}(watts) and the relevant quantities are defined as follows:

$A(m^2)$ = total area of the FS covered by the sheaths;

γ = the angle between the field line and the FS surface(estimated along the radial co–ordinate);

$n_{io}(m^{-3})$ = the local density at the FS;

$\phi_o(V)$ = rectified sheath potential = $C_{sh}V_o$ where

V_o = AC voltage (0 to peak) across the rf sheaths and $C_{sh} \approx 0.6$ is a factor resulting from the numerical sheaths simulations[12];

$T_e(eV)$ = local electron temperaure at the FS;

μ = ion mass divided by the proton mass and the sum is over species. Because D^+ gives the dominant contribution, we can set Z = 1 and neglect the sum. Using relation between rectified potential and sheath voltage[12] we obtain

$$P_{FS} = 0.9 \times 10^{-15}\, A \sin\gamma\, n_{io}\, V_o\, (T_e/\mu)^{1/2} \qquad (2)$$

where the sheath voltage is defined

$$V_o = (c\, V_l/L_{Ap})\, (L_{At}/2) \tan\alpha.$$

Here V_l is the maximum voltage measured on the transmission line, c ≈1.4 is the transmission line/antenna transformation factor[15] and L_{Ap} and L_{At} are the poloidal and toroidal dimensions of antenna screen. The factor 1/2 comes from computing the voltage of a "typical" field line connecting two points at the front face of FS. For details of the FS geometry the reader is refered to discussion and drawings in ref.[5].

Consider now, as an example, a reversed field case from the data set plotted in Fig.5, where the total coupled RF power was ≈ 6 MW. This implies, with 6 antennas

being operational, 1 MW per antenna. Given the coupling resistance $R_c \approx 5\ \Omega$, L_{At} = 0.4 m. L_{Ap} =1.4 m, α = 22 degrees the resulting sheath voltage $V_0 \approx 1.5$ kV and the Eq.(2) give

$$P_{FS} = \frac{n_{io}}{(10^{17} m^{-3})} \times 110\ kW \qquad (3)$$

Electron temperature T_e=100 eV and "typical" γ = 10 degrees are assumed. Thus 400 kW of dissipated power at the FS screen would require a local value of density at the FS of 3.6 x 10^{17} m^{-3}. Because the dissipated power fraction P_{FS} is a linear function of P_{RF} it follows that $n_{io}^2 T_e \propto P_{RF}^2$. The enhanced particle flux into the FS was observed earlier[16] and the necessity for introduction of such flux in the modelling of impurity generation was discussed in previous publications[5,6]. It should be noted here, that in the dipole antenna phasing the dissipation at the screen is neither observed nor expected. In the monopole phasing and the normal direction of the field the dissipation should be reduced by roughly factor 5.

When the power per antenna exceeded 1.5 MW, in the reversed field case, sudden arcing across the FS occurred. At that instant the voltage V_0 was in the range $\approx$2 kV. Associated with the arc a large release of beryllium from the FS was recorded(telescope with BeI filter) as shown in Fig. 6. The arc lasted for the duration of the beryllium spike. Several cases of arcs, similar to the one documented in Fig.6, were observed. The CCD camera view(BeI filter), intercepting the same FS as the BeI telescope, has shown that the arc strikes across the FS along the direction of the static magnetic field $\vec{B}(a)$. During one case, a poloidal displacement of the arc along the antenna screen was observed. As can be seen from the coupling resistance evolution in Fig.6 the antenna resistive loading is not affected by the arc. However the reactive loading of the antennna current straps has changed and the corresponding adjustment of the generator frequency can be clearly seen. The generator is operating in the automatic matching mode[17].

4.0 Discussion.

The installement of all beryllium FS on JET antennas led to ellimination of the RF–specific impurity influxes from the screens with antennas phased as dipoles. The assessment of the new screens by the series of measurements presented in this paper has shown that the basic mechanism for the impurity production at the screen is understood[5,6,7] and thus the influx from the screen scales with the antenna voltage, edge density, antenna phasing and FS/$\vec{B}$(a) angle as expected. The open screen works faultlessly and as a result a large number of different high performance operation regimes with ICRF heating are now possible[2]. Operating the JET RF system at large FS/$\vec{B}$(a) angles proved to be difficult only in monopole phasing with a large fraction of power dissipated at the screen. It can be concluded that by minimising the RF–enhanced sheath at the FS surface by the proper design of the antenna and the choice of the low Z material for the screen will elliminate the RF–specific impurity effects which, in a large scale device like JET or the next step device, are taking place at the antenna screen due to the localization of the high amplitude RF fields close to the powered antennas. To summarise, a properly designed antenna should include following features:

1)FS elements should be as closely as possible aligned to the boundary magnetic field

2)density at the FS should be minimised by the use of the side protection tiles

3)antennas should preferably be operated in the dipole(out of phase) phasing of the current straps

4)antenna voltage should be minimised by working at the lowest possible power density

5)low Z material, such as beryllium, should be used because it has relatively low selfsputtering coefficient at the energies around 0.5–1keV.

In view of the JET results the impurity problems, associated in earlier days with the ICRF heating, should not pose any difficulty in the next step device. Even in the case of the fast wave current drive, when the antennae are phased at a large range of the angles, the influx from the FS should not pose any difficulty. If the tokamak is to be

operated in the AC mode, with the plasma current changing direction during each subsequent pulse, the compromise on the FS/$\vec{B}$(a) angle should be reached,i.e., $\theta_0=0^o$.

Acknowledgements.

We wish to thank our colleagues in the JET team, especially the tokamak operating teams and those operating the diagnostics used in the experiments reported in this paper.

References.

[1] REBUT, P.H., and The JET Team(1990) Proc.13th Int. Conf. on Plasma Phys. and Contr. Nucl. Fusion Res. Washington, paper IAEA–CN–53/A–1–2.

[2] JACQUINOT, J. and JET Team,(1991), Proc 18th Europ. Conf. on Contr. Fusion and Plasma Heating, Berlin, to appear in Plasma Phys. and Contr. Fusion.

[3] BEHRINGER, K., DENNE, B., FORREST, M. et al., Contr. Fus. and Plasma Heating(Proc. 13th Eur. Conf. Schliersee, 1986)Vol.10C, Part I, Europ. Phys. Soc., p.176.

[4] BUREŠ, M., BRINKSHULTE, H., JACQUINOT, J. et al., Plasma Phys. and Contr. Fus., Vol.30, No.2(1988)149.

[5] D'IPPOLITO, D., MYRA, J., BUREŠ, M. and J. JACQUINOT, Plasma Phys. and Contr. Fus., Vol.33, No.7,(1991)607.

[6] BUREŠ, M., JACQUINOT, J., LAWSON, K. et al., JET Report JET–P(90)49, accepted for publication in Plasma Phys. and Contr. Fus.

[7] PERKINS, F.W.(1989) Nucl.Fusion 29,p.277.

[8] WALKER C.I., BRINKSHULTE, H., BUREŠ, M. et al., Fusion Technology 1988, Elsevier Science Publishers B.V., (1989)444.

[9] ERENTS, S.K., CLEMENT, S., HARBOUR, P. et al., Journal Nucl. Mater. 176 & 177(1990)301.

[10] BUREŠ, M., CAMPBELL, D., GOTTARDI, N. et al., submitted for publication in Nucl. Fus.

[11] JACQUINOT, J. and JET Team,(1988), Plasma Phys. and Contr. Fusion, Vol.30, No.11, p.1467.

[12] MYRA, J.R., D'IPPOLITO, D., GERVER, M. J. Nucl.Fusion 30,(1990)845, and also Lodestar Res. Corp. Rep. No.LRC–89–5(1989).

[13] D'IPPOLITO, D., MYRA, J., BUREŠ, M. et al.,Fusion Engrg. Des. 12, p.209.

[14] CHODURA R. and NEUHAUSER J., Contr. Fusion and Plasma Heating, (Proc. 16th Europ. Conf. Venice, 1989)Vol.13B, Part III, Europ. Phys. Soc., p.1089.

[14] EVRARD M.P., BHATNAGAR, V., BUREŠ, M. et al., Contr. Fus. and Plasma Heating(Proc. 13th Eur. Conf. Schliersee, 1986)Vol.10C, Part II, Europ. Phys. Soc., p.133.

[16] TAGLE J.A., LAUX, M., CLEMENT, S. et al., Fusion Engrg. Des. 12, p.217.

[17] BOSIA, G., LAMONT, B., SIBLEY, A. et al., JET–P(90)56, Vol.I, To appear in Proc. 16th SOFT, London(1990).

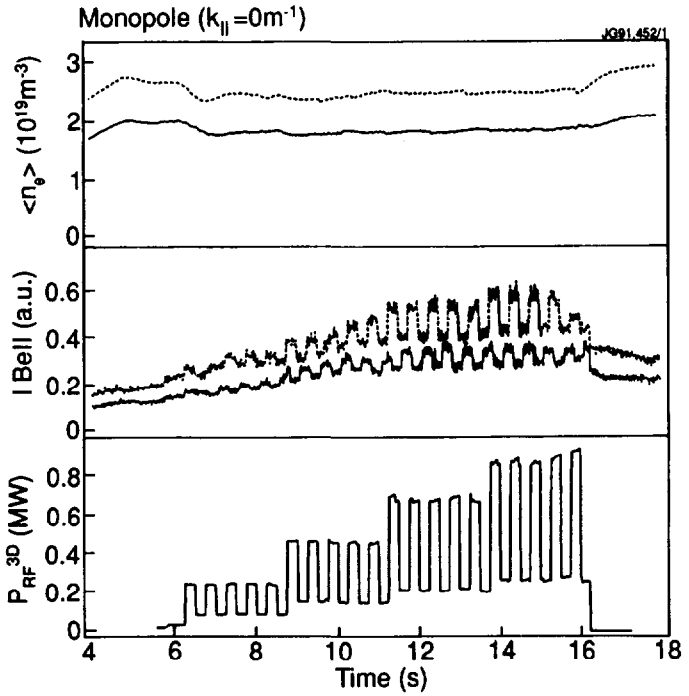

Fig.1 Plasma density, intensity of BeII line and the RF power as a function of time in two different discharges. The BeII signal is monitored along the line of sight interscepting the Faraday screen of the antenna 3D.

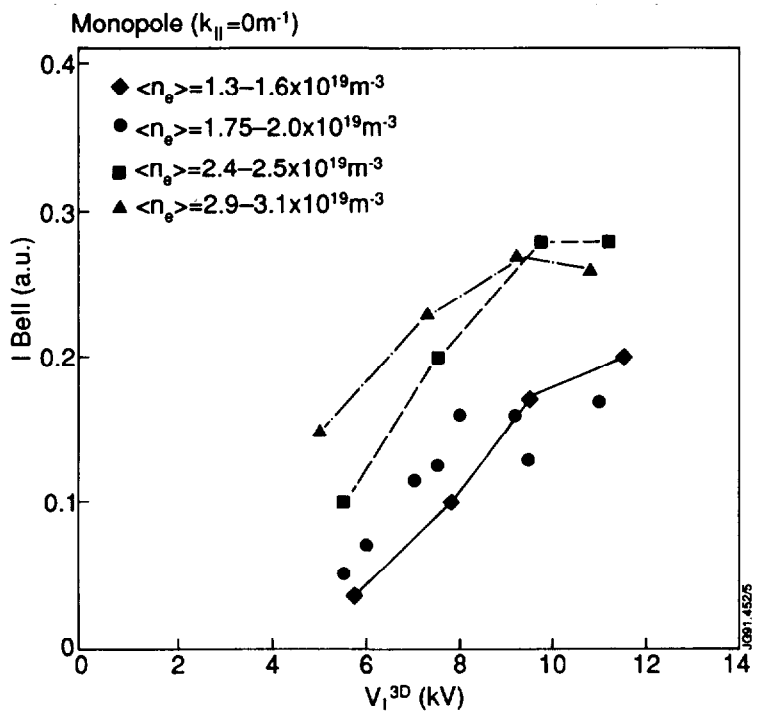

Fig.2 BeII signal at the Faraday screen of 3D antenna at different plasma densities as a function of antenna line voltage(measured on the transmission line).

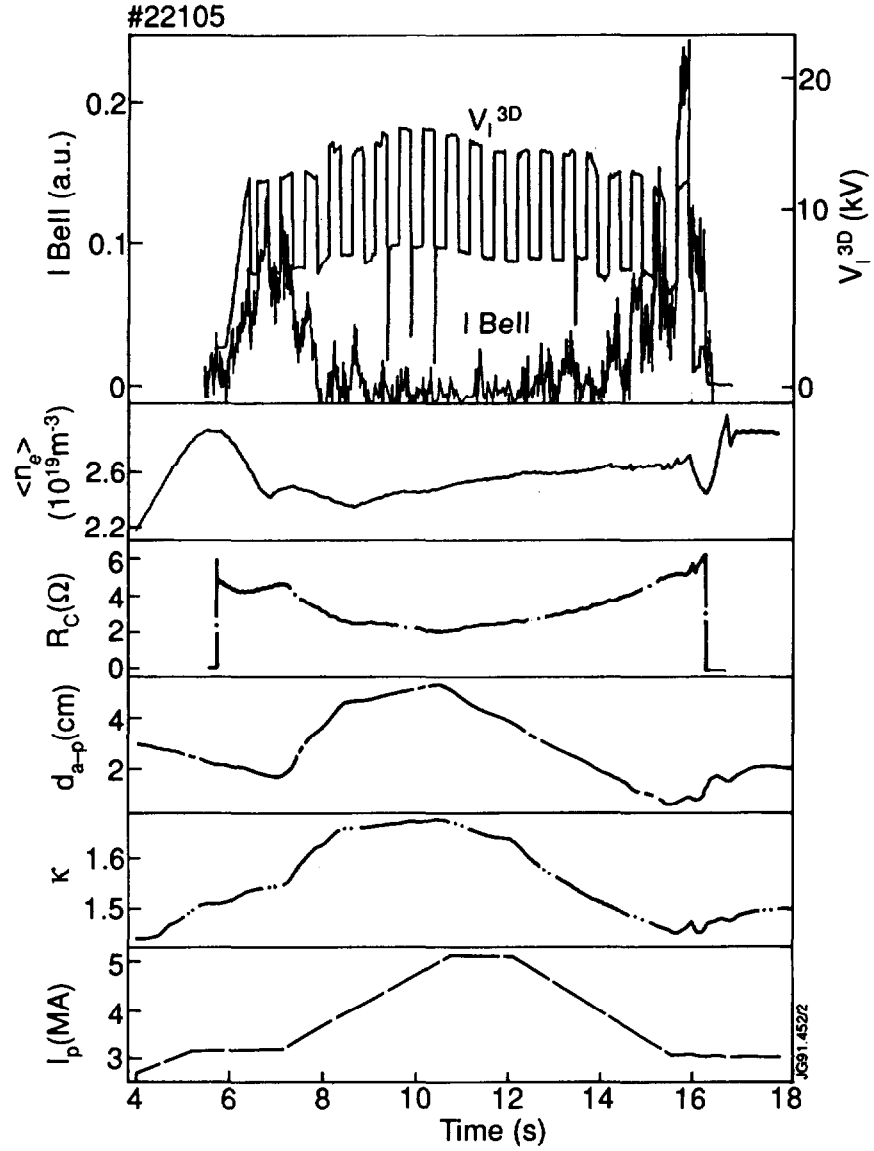

Fig.3 Intensity of BeII signal measured at the Faraday screen of 3D antenna and the antenna line voltage during the ramp of plasma current from 3 to 5 MA and back to 3 MA. Plasma density, coupling resistance, distance antenna–plasma and the plasma elongation are also shown.

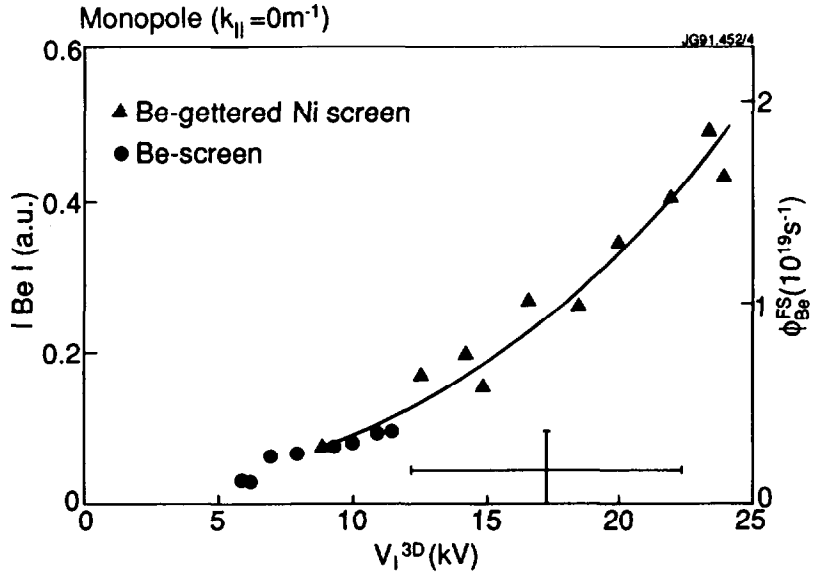

Fig.4 Influx of neutral beryllium from the Faraday screen as a function of antenna line voltage. The range of values indicated separately in the figure refers to the influxes monitored during the late part of the experimental campaign when the screens were in situ covered by a layer of carbon.

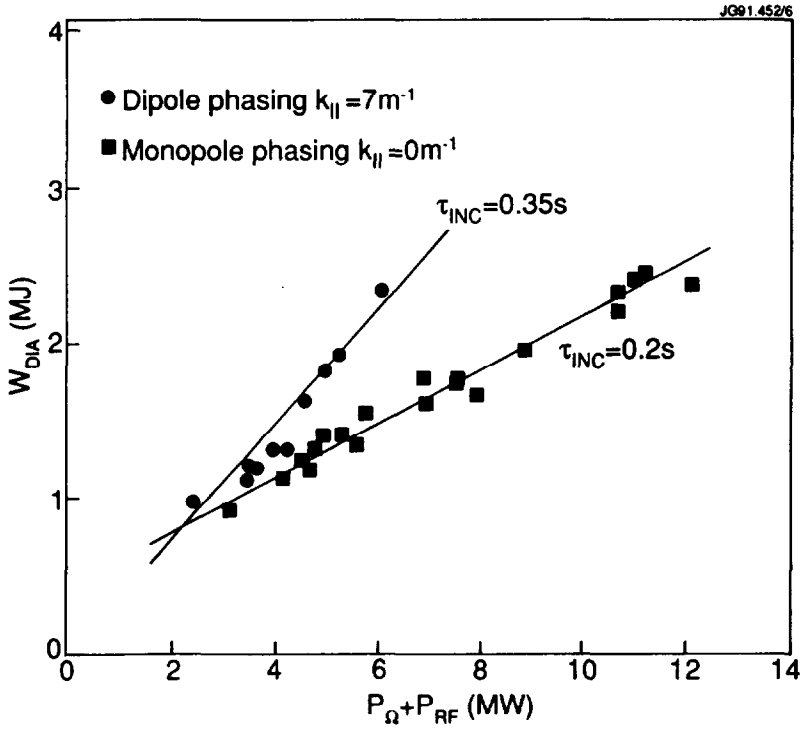

Fig.5 Plasma stored energy as a function of input power with dipole and monopole phasing. During these discharges the direction of toroidal field was reversed and the angle between the screen elements and the magnetic field in the boundary was $\alpha \approx 22$ degrees.

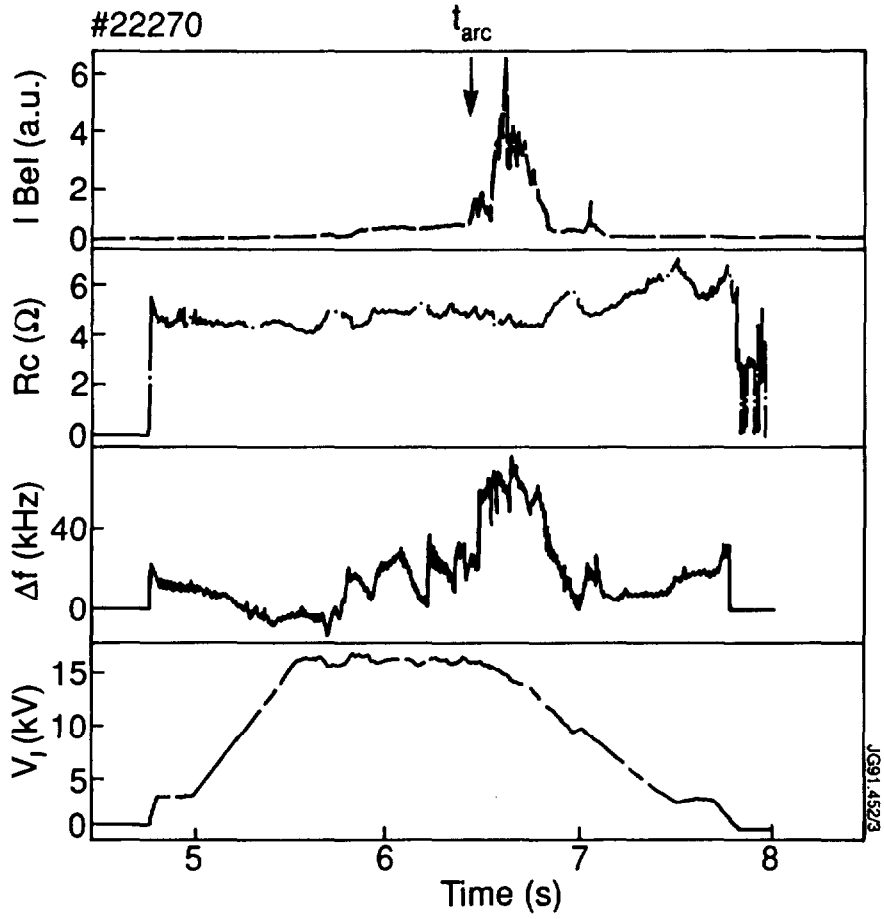

Fig.6 Large influx of beryllium from the antenna screen due to an arc across the screen. Coresponding coupling resistance, generator frequency response and the antenna line voltage are also shown. The antennas are phased as monopoles and the toroidal field is reversed.

Appendix I

THE JET TEAM

JET Joint Undertaking, Abingdon, Oxon, OX14 3EA, U.K.

J.M. Adams[1], H. Altmann, A. Andersen[14], P. Andrew[18], M. Angelone[29], S.A. Arshad, W. Bailey, P. Ballantyne, B. Balet, P. Barabaschi, R. Barnsley[2], M. Baronian, D.V. Bartlett, A.C. Bell, I. Benfatto[5], G. Benali, H. Bergsaker[11], P. Bertoldi, E. Bertolini, V. Bhatnagar, A.J. Bickley, H. Bindslev[14], T. Bonicelli, S.J. Booth, G. Bosia, M. Botman, D. Boucher, P. Boucquey, P. Breger, H. Brelen, H. Brinkschulte, T. Brown, M. Brusati, T. Budd, M. Bures, T. Businaro, P. Butcher, H. Buttgereit, C. Caldwell-Nichols, D.J. Campbell, P. Card, G. Celentano, C.D. Challis, A.V.Chankin[23], D. Chiron, J. Christiansen, C. Christodoulopoulos, P. Chuilon, R. Claesen, S. Clement, E. Clipsham, J.P. Coad, M. Comiskey[4], S. Conroy, M. Cooke, S. Cooper, J.G. Cordey, W. Core, G. Corrigan, S. Corti, A.E. Costley, G. Cottrell, M. Cox[7], P. Cripwell, H. de Blank[15], H. de Esch, L. de Kock, E. Deksnis, G.B. Denne-Hinnov, G. Deschamps, K.J. Dietz, S.L. Dmitrenko, J. Dobbing, N. Dolgetta, S.E. Dorling, P.G. Doyle, D.F. Düchs, H. Duquenoy, A. Edwards, J. Ehrenberg, A. Ekedahl, T. Elevant[11], S.K. Erents[7], L.G. Eriksson, H. Fajemirokun[12], H. Falter, D. Flory, J. Freiling[15], C. Froger, P. Froissard, K. Fullard, M. Gadeberg, A. Galetsas, D. Gambier, M. Garribba, P. Gaze, R. Giannella, A. Gibson, R.D. Gill, A. Girard, A. Gondhalekar, C. Gormezano, N.A. Gottardi, C. Gowers, B.J. Green, R. Haange, G Haas, A. Haigh, G. Hammett[6], C.J. Hancock, P.J. Harbour, N.C. Hawkes[7], P. Haynes[7], J.L. Hemmerich, T. Hender[7], F.B. Herzog, R.F. Herzog, J. Hoekzema, J. How, M. Huart, L Hughes, T.P. Hughes[4], M. Hugon, M. Huguet, A. Hwang[7], B. Ingram, M. Irving, J. Jacquinot, H. Jaeckel, J.F. Jaeger, G. Janeschitz[13], S. Jankowicz[22], O.N. Jarvis, F. Jensen, E.M. Jones, L.P.D.F. Jones, T.T.C. Jones, J-F. Junger, E. Junique, A. Kaye, B.E. Keen, M. Keilhacker, G.J. Kelly, W. Kerner, R. Konig, A. Konstantellos, M. Kovanen[20], G. Kramer[15], P. Kupschus, R. Lässer, J.R. Last, B. Laundy, L. Lauro-Taroni, K. Lawson[7], M. Lennholm, A. Loarte, R. Lobel, P. Lomas, M. Loughlin, C. Lowry, B. Macklin, G. Maddison[7], G. Magyar, W. Mandl[13], V. Marchese, F. Marcus, J. Mart, E. Martin, R. Martin-Solis[8], P. Massmann, G. McCracken[7], P. Meriguet, P. Miele, S.F. Mills, P. Millward, R. Mohanti[17], P.L. Mondino, A. Montvai[3], S. Moriyama[28], P. Morgan, H. Morsi, G. Murphy, M. Mynarends, R. Myrnäs[16], C. Nardone, F. Nave[21], G. Newbert, M. Newman, P. Nielsen, P. Noll, W. Obert, D. O'Brien, J. O'Rourke, R. Ostrom, M. Ottaviani, M. Pain, F. Paoletti, S. Papastergiou, D. Pasini, A. Peacock, N. Peacock[7], D. Pearson[12], R. Pepe de Silva, G. Perinic, C. Perry, M. Pick, R. Pitts[7], J. Plancoulaine, J-P. Poffé, F. Porcelli, L. Porte[19], R. Prentice, S. Puppin, S. Putvinsko[23], G. Radford[9], T. Raimondi, M.C. Ramos de Andrade, P-H. Rebut, R. Reichle, E. Righi, F. Rimini, D. Robinson[7], A. Rolfe, R.T. Ross, L. Rossi, R. Russ, P. Rutter, H.C. Sack, G. Sadler, G. Saibene, J.L. Salanave, G. Sanazzaro, A. Santagiustina, R. Sartori, C. Sborchia, P. Schild, M. Schmid, G. Schmidt[6], B. Schunke, S.M. Scott, A. Sibley, R. Simonini, A.C.C. Sips, P. Smeulders, R. Stankiewicz[27], M. Stamp, P. Stangeby[18], D.F. Start, C.A. Steed, D. Stork, P.E. Stott, T.E. Stringer, P. Stubberfield, D. Summers, H. Summers[19], L. Svensson, J.A. Tagle[21], A. Tanga, A. Taroni, A. Tesini, P.R. Thomas, E. Thompson, K. Thomsen, J.M. Todd, P. Trevalion, B. Tubbing, F. Tibone, E. Usselmann, H. van der Beken, G. Vlases, M. von Hellermann, T. Wade, C. Walker, R. Walton[6], D. Ward, M.L. Watkins, M.J. Watson, S. Weber[10], J. Wesson, T.J. Wijnands, J. Wilks, D. Wilson, T. Winkel, R. Wolf, B. Wolle[24], D. Wong, C. Woodward, Y. Wu[25], M. Wykes, I.D. Young, L. Zannelli, Y. Zhu[26], W. Zwingmann.

PERMANENT ADDRESSES

1. UKAEA, Harwell, Didcot, Oxon, UK.
2. University of Leicester, Leicester, UK.
3. Central Research Institute for Physics, Academy of Sciences, Budapest, Hungary.
4. University of Essex, Colchester, UK.
5. ENEA-CNR, Padova, Italy.
6. Princeton Plasma Physics Laboratory, New Jersey, USA.
7. UKAEA Culham Laboratory, Abingdon, Oxon, UK.
8. Universidad Complutense de Madrid, Spain.
9. Institute of Mathematics, University of Oxford, UK.
10. Freien Universität, Berlin, F.R.G.
11. Swedish Energy Research Commission, S-10072 Stockholm, Sweden.
12. Imperial College of Science and Technology, University of London, UK.
13. Max Planck Institut für Plasmaphysik, Garching bei München, FRG.
14. Risø National Laboratory, Denmark.
15. FOM Instituut voor Plasmafysica, 3430 Be Nieuwegein, The Netherlands.
16. University of Lund, Sweden.
17. North Carolina State University, Raleigh, NC, USA
18. Institute for Aerospace Studies, University of Toronto, Downsview, Ontario, Canada.
19. University of Strathclyde, 107 Rottenrow, Glasgow, UK.
20. Nuclear Engineering Laboratory, Lapeenranta University, Finland.
21. CIEMAT, Madrid, Spain.
22. Institute for Nuclear Studies, Otwock-Swierk, Poland.
23. Kurchatov Institute of Atomic Energy, Moscow, USSR
24. University of Heidelberg, Heidelberg, FRG.
25. Institute for Mechanics, Academia Sinica, Beijing, P.R. China.
26. Southwestern University of Physics, Leshan, P.R. China.
27. RCC Cyfronet, Otwock Swierk, Poland.
28. JAERI, Naka Fusion Research Establishment, Ibaraki, Japan.
29. ENEA, Frascati, Italy.

At 1st June 1991